Polym. Bull. (2011) 67:815–830
DOI 10.1007/s00289-011-0456-5

ORIGINAL PAPER

Changes in the crystallinity and mechanical properties of poly(L-lactic acid)/poly(butylene succinate-*co*-L-lactate) blend with annealing process

P. M. Chou · M. Mariatti · A. Zulkifli · M. Todo

Received: 25 July 2010 / Revised: 3 January 2011 / Accepted: 8 February 2011 /
Published online: 17 February 2011

Abstract Biodegradable polymer blends of poly(L-lactic acid) (PLLA) and poly(butylene succinate-*co*-L-lactate) (PBSL) at various blending ratios are prepared. The blending of PLLA with PBSL results in an increase in the ductility and thermal stability of the blend. However, flexural strength and modulus, as well as loss modulus, decrease with an increase in PBSL content. Annealing is employed to increase blend crystallinity and subsequently improve the mechanical properties of the PLLA/PBSL blend. The influences of annealing time on the crystal modification, thermal properties, and mechanical properties of the PLLA/PBSL blend are investigated by X-ray diffraction (XRD), differential scanning calorimetry (DSC), and three-point bending test, respectively. Crystalline peaks are found in the XRD patterns of all annealed samples. DSC analysis reveals that the degree of crystallinity is enhanced with an increase in annealing time. The flexural modulus also increases with annealing time due to the change in crystalline phases. However, longer periods of annealing, especially over 20 h, result in thermal degradation and subsequently reduce the modulus value of the PLLA/PBSL blend.

Keywords Poly(L-lactic acid) (PLLA) · Poly(butylene succinate-*co*-L-lactate) (PBSL) · Annealing · Crystallization behavior

P. M. Chou · M. Mariatti (✉) · A. Zulkifli
School of Materials and Mineral Resources Engineering, Universiti Sains Malaysia, Engineering Campus, 14300 Pulau Pinang, Malaysia
e-mail: mariatti@eng.usm.my

M. Todo
Research Institute for Applied Mechanics, Kyushu University, Fukuoka 812-0003, Japan

Introduction

The greenhouse effect, caused by the widespread consumption of petroleum-based polymers and plastics, has spurred the development of biodegradable or environment-friendly materials. Biopolymers derived from various natural botanical resources, such as protein and starch, have been regarded as substitutes for petrochemical-based plastics because they are abundant, renewable, and biodegradable [1, 2]. In this context, poly(L-lactic acid) (PLLA) is one of several biodegradable and biocompatible semi-crystalline polymers that can be derived from renewable agricultural raw materials. Its mechanical properties are comparable to those of commercially available engineering polymers, making it suitable for use in biomedical applications, such as controlled-release devices, absorbable sutures, and orthopedic implants [3].

Nevertheless, PLLA possesses several limitations, such as poor thermal stability, relatively high cost, and brittleness [4]. These limitations can be resolved to a certain extent by blending PLLA with polymers that exhibit ductile impact fracture behaviors, such as poly(ε-caprolactone) (PCL) [5], poly(butylene succinate) (PBS) [6], and poly(hydroxyl ester ether) [7]. According to Shibata et al. [8], the tensile strength and modulus of PLLA/PBS blend approximately followed the rule of mixture. Moreover, the elongation at break of the blends was higher than that of the neat PLLA or PBS. In the previous work conducted by Bhatia et al. [9], viscosities of PLA increased with the addition of PBS above 50 wt% while, the viscosities of the blends having 10 and 20 wt% PBS content were in between the neat polymers, indicating that below 20 wt% of PBS, PLA/poly(butylene succinate-*co*-L-lactate) (PBSL) blends showed miscibility and beyond that they became immiscible. Apart from that, Park and Im [10] reported that the addition of PBS improved the crystallinity of PLLA. Similar findings have been documented by Yokohara and Yamaguchi [11], whereby the crystallization of PLA was enhanced by blending with PBS.

In general, the crystallization behavior of semicrystalline polymers has vital effects on their physical, mechanical, and thermal properties. The crystalline structure of a semicrystalline polymer, such as PLLA, has been shown to greatly depend on its thermal history and pretreatment [12]. Tsuji and Ikada [13] studied the effects of annealing on the properties and morphologies of solution-cast PLA films. It was found that both tensile strength and Young's modulus were increased after annealing. In addition, Huda et al. [14] reported that an increase in the storage modulus of PLLA film was observed after annealing process as the crystallization of PLLA films was increased by annealing.

The present work focuses on the determination of the optimum blending ratio of PLLA/PBSL blends. Changes in the crystallinity of the PLLA/PBSL blend are considered when the optimum blend is annealed at 100 °C for different time periods. The effects of annealing time on the crystalline structure, as well as the thermal properties, of the PLLA/PBSL blends are characterized by X-ray diffraction (XRD) and differential scanning calorimetry (DSC). The three-point bending test was performed to measure flexural strength and modulus. The fracture surface and morphology of the blend are then revealed under field emission scanning electron microscopy (FESEM).

Experimental

Materials

PLLA pellets (Lacty 5000) with a weight-average molecular weight of 1.45×10^5 were supplied by Shimadzu Co. Ltd. PBSL pellets with a weight-average molecular weight of 1.47×10^5 were obtained from Mitsubishi Chemical Corp. Both PLLA and PBSL pellets were used as received.

Blend preparation

Samples with blending ratios of 100/0, 75/25, 25/75, and 0/100 were prepared by melt mixing PLLA and PBSL pellets for 7 min using a Haake internal mixer with a twin screw speed of 50 rpm at 170 °C. Before blending, the PLLA and PBSL pellets were dried in a vacuum oven for 24 h at 80 °C. After blending, the specimens were hot pressed for 5 min at 180 °C and 10 MPa. This was followed by cooling to room temperature. To study the influences of annealing time on the mechanical properties and crystalline structure of the blends, hot-pressed specimens were put in a vacuum oven at 100 °C for varying annealing time periods of 5, 10, 15, and 20 h. According to a previous study conducted by Kobayashi and Kogo [15], 100 °C is the optimum annealing temperature in which the crystallinity of PLLA saturates. The specimens were then sealed in plastic bags and kept in a desiccator while awaiting characterization.

Differential scanning calorimetry (DSC)

The glass transition temperature (T_g), crystallization temperature (T_c), and melting temperature (T_m) of the PLLA/PBSL blend specimens were determined using a Perkin-Elmer Pyris 1 differential scanning calorimeter (DSC) that was calibrated using indium as the standard. The specimens were first heated from −50 to 200 °C at a heating rate of 10 °C/min and held at 200 °C for 3 min. The specimens were then cooled from 200 to −50 °C at a cooling rate of 20 °C/min to diminish thermal history. This was followed by a second scan from −50 to 200 °C at 10 °C/min. The degree of crystallinity (X_c) of PLLA in the blends was evaluated using Eq. 1:

$$X_c(\%) = \frac{\Delta H_m - \Delta H_c}{x \times \Delta H_m^{\theta}} \times 100, \quad (1)$$

where ΔH_m is its enthalpy of melting, ΔH_c is the enthalpy of crystallization of PLLA, ΔH_m^{θ} is its enthalpy of fusion (i.e., 93 J/g as reported by Fischer et al. [16]), and x is its weight fraction in the blend.

Thermal gravimetric analysis (TGA)

A Pyris Diamond thermal gravimetric analyzer (TGA) was used to measure the thermal stability and decomposition temperature of the test samples. This was conducted by monitoring the weight change that occurred as a specimen was heated.

Measurements were carried out in an inert atmosphere, and weight loss was recorded as a function of increasing temperature. TGA was run from 30 to 650 °C at a heating rate of 10 °C/min.

Dynamic mechanical analysis (DMA)

The DMA was performed with a Mettler-Toledo dynamic mechanical analyzer Model 861 in dual cantilever mode. The scan was run from −100 to 100 °C at a frequency of 1 Hz. The storage modulus, tan δ, and loss modulus of the specimens were recorded as a function of temperature.

Flexural test

The three-point bending test was carried out using Instron Universal Testing Machine Model 3366 at a cross-head speed of 10.00 mm/min and a span length of 50 mm. The specimens were cut into bars of rectangular cross sections with dimensions of 100 mm × 12.7 mm × 3 mm as recommended by ASTM D790-03 [17]. The flexural strength and modulus were computed based on the average results of five flexural specimens.

FESEM observations

The morphology of the poly(lactic acid) blends was examined using a field emission scanning electron microscope (FESEM) Model Supra 35 VP Zeiss. The fracture surfaces were coated with gold before the examination.

X-ray diffraction (XRD) analysis

X-ray diffraction (XRD) analyses of the annealed and unannealed specimens were performed on a Bruker D8 powder diffractometer equipped with a Cu K_{α} radiation source. The analysis was carried out at 40 kV and 30 mA from 10° to 45° at a 2θ scanning rate of 1°/min.

Results and discussion

PLLA/PBSL blending ratio

Thermal properties

Figure 1 displays the DSC thermograms of virgin PLLA, PBSL, and the PLLA/PBSL blends. As seen in Fig. 1, the PLLA/PBSL blends exhibited two endothermic peaks at about 110 and 174 °C, which correspond to the melting point (T_m) of neat PBSL and PLLA, respectively. The melting point of PLLA decreased slightly with an increase in PBSL content. In addition, the PLLA/PBSL blends showed two glass transition temperatures at about −33 and 57 °C, representing the glass transition

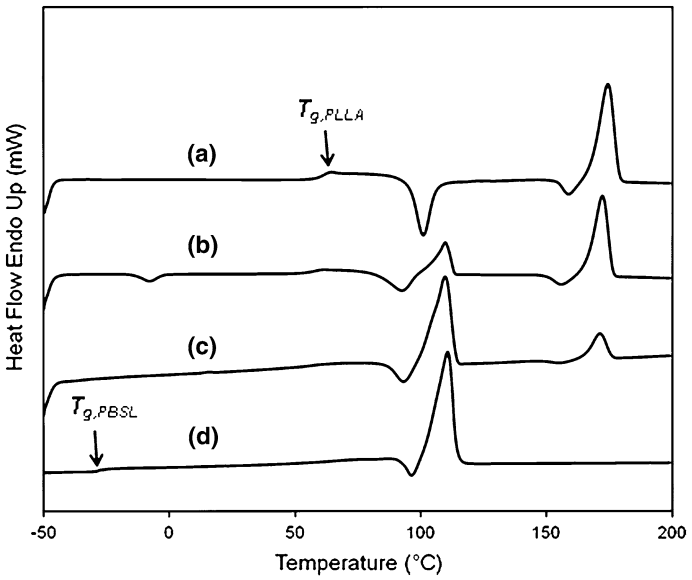

Fig. 1 DSC thermograms of **a** neat PLLA, **b** 75/25 PLLA/PBSL blend, **c** 25/75 PLLA/PBSL blend, and **d** neat PBSL

Table 1 Thermal properties and degree of crystallinity (X_c) of PLLA/PBSL blends

PLLA/PBSL composition	$T_{g,PBSL}$ (°C)	$T_{g,PLLA}$ (°C)	$T_{c,PLLA}$ (°C)	$\Delta H_{c,PLLA}$ (J/g)	$T_{m,PLLA}$ (°C)	$\Delta H_{m,PLLA}$ (J/g)	$X_{c,PLLA}$ (%)
100/0	–	61.58	100.96	−26.98	174.41	55.09	88.24
75/25	−33.42	57.75	92.49	−12.31	172.28	40.33	75.47
25/75	−33.88	56.26	93.15	−8.37	171.21	14.51	0.98
0/100	−33.84	–	–	–	–	–	–

temperature (T_g) of PBSL and PLLA, respectively. Although these T_g's cannot be seen clearly from Fig. 1 due to their very weak intensities, the PLLA/PBSL blends with blending ratios of 75/25 and 25/75 have similar T_g's. These T_g's shifted towards each other, suggesting that the blends are partially miscible [18]. In the DSC thermogram of neat PLLA, two exothermic peaks were observed at about 100 °C and just before the melting point of PLLA. The first exothermic peak was probably due to the cold crystallization of PLLA [19], whereas the second exothermic peak was attributed to the recrystallization of the lower perfection crystals of PLLA into higher perfection crystals. Similar exothermic peaks were observed in the 75/25 PLLA/PBSL blend. However, due to the small amount of PLLA in the 25/75 PLLA/PBSL blend, the exothermic trend was not obviously shown in this blend. This is in agreement with the findings reported by Zhang et al. [20]. The thermal properties and degree of crystallinity (X_c) of PLLA/PBSL blends are summarized in Table 1.

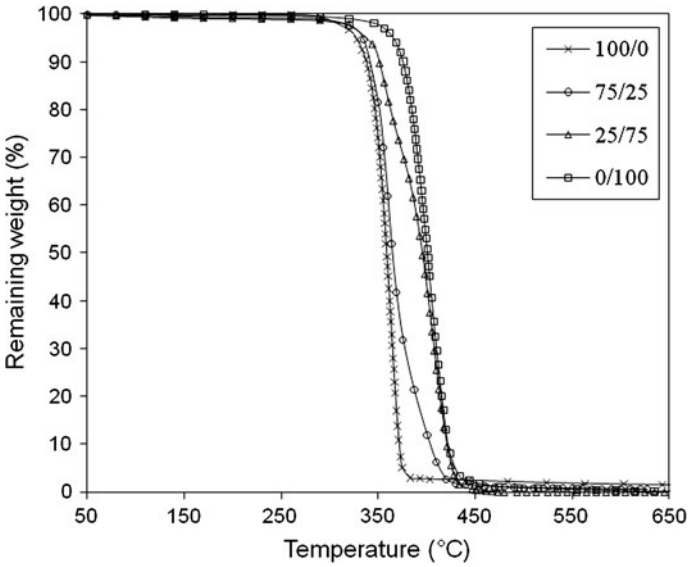

Fig. 2 TGA curves of neat PLLA, PBSL, and PLLA/PBSL blends

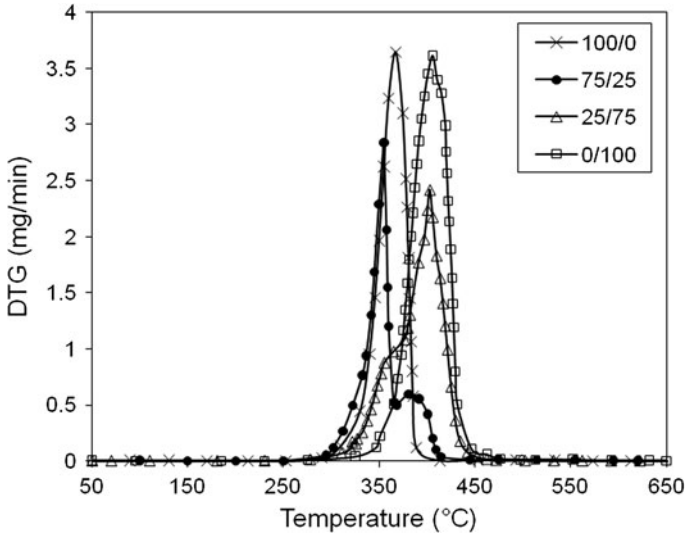

Fig. 3 DTG curves of neat PLLA, PBSL, and PLLA/PBSL blends

Typical weight loss (TG) and derivative of weight loss (DTG) curves of PLLA, PBSL, and PLLA/PBSL blends were presented in Figs. 2 and 3, respectively. Table 2 presents the degradation temperature and residue of the samples. From DTG curves, the maximum temperature of weight loss was also noted. The mass loss of neat PBSL began at 350 °C and reached to maximum at 405 °C. However,

Table 2 Measurement of degradation temperature and residue of virgin PLLA, PBSL, and PLLA/PBSL blends

PLLA/PBSL composition	Decomposition temperature (°C)	Temperature at 5% weight loss (°C)	Temperature at 20% weight loss (°C)	Residue at 650 °C (%)
100/0	346.5	326.9	346.6	0.9
75/25	352.3	334.2	351.0	0.4
25/75	367.1	339.7	362.6	0.0
0/100	378.0	365.6	384.9	0.0

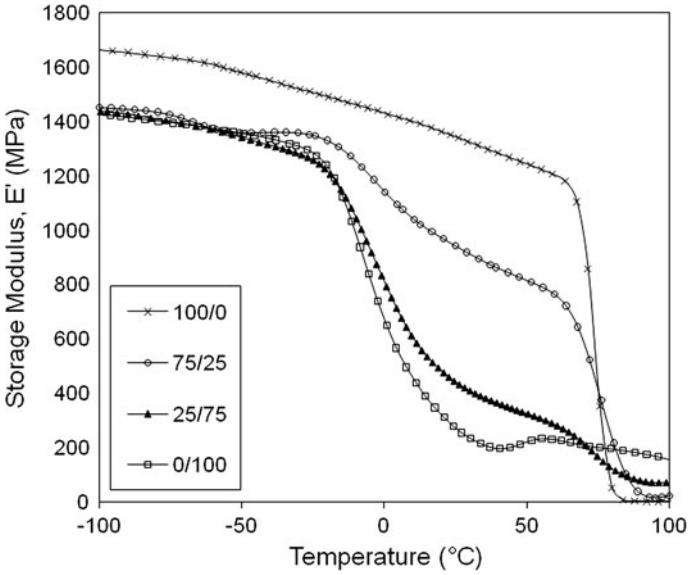

Fig. 4 Storage modulus curves of neat PLLA, PBSL, and the blends

the mass loss of virgin PLLA started at 320 °C and reached to maximum at 367 °C. The neat PBSL exhibited better thermal stability than that of PLLA. The TG curves of both PLLA and PBSL also indicated one reaction stage which was reflected as single peak in the DTG curves as shown in Fig. 3. However, PLLA/PBSL blends degraded in two steps. This was evidenced by the appearance of distinct peaks in DTG thermograms. Two distinct reaction peaks at around 350 and 410 °C were identified in the DTG thermograms of the blends. These peaks were attributed to the thermal degradation of PLLA and PBSL, respectively. This behavior showed that the thermal degradation reaction mechanism of PLLA/PBSL blends was the same as the PLLA and PBSL homopolymers. The TGA results indicated that partially miscible blends were achieved and in agreement with the findings reported by Zhang et al. [21] and Kong et al. [22].

Dynamic mechanical analysis

Figure 4 presents the storage modulus (E') of PLLA, PBSL, and the PLLA/PBSL blends as a function of temperature. The neat PLLA exhibited the highest storage modulus at −100 °C (1664.31 MPa). In addition, the dramatic drop in storage modulus of the neat PLLA is the steepest. The introduction of PBSL into the blends resulted in a reduction in storage modulus because the value of storage modulus of PBSL is lower than that of PLLA.

The temperature dependence of the loss moduli (E'') of neat PLLA, PBSL, and the PLLA/PBSL blends is demonstrated in Fig. 5. It was found that the peak based on the loss modulus decreased with an increase in PBSL, which possesses a lower value of loss modulus compared with PLLA. The peak temperature of the loss modulus corresponds to the α relaxation related to glass transition temperature (T_g) of the samples [23]. All PLLA blends exhibited two peaks at about the α relaxation related to T_g of PBSL and PLLA. This implies that the blends consisted of two separate phases, the PLLA-rich and PBSL-rich phases. In other words, PBSL is partially miscible with PLLA. These results are consistent with the DSC analysis presented in the previous section. However, the value of α relaxation related to glass transition obtained from DMA is higher than the glass transition temperature obtained from DSC analysis. This may be attributed to the different measuring mechanisms between DSC and DMA [24].

Flexural properties

The flexural stress–strain curves of neat PLLA, PBSL, and the PLLA/PBSL blends are presented in Fig. 6. The toughness of the samples can be evaluated from the area

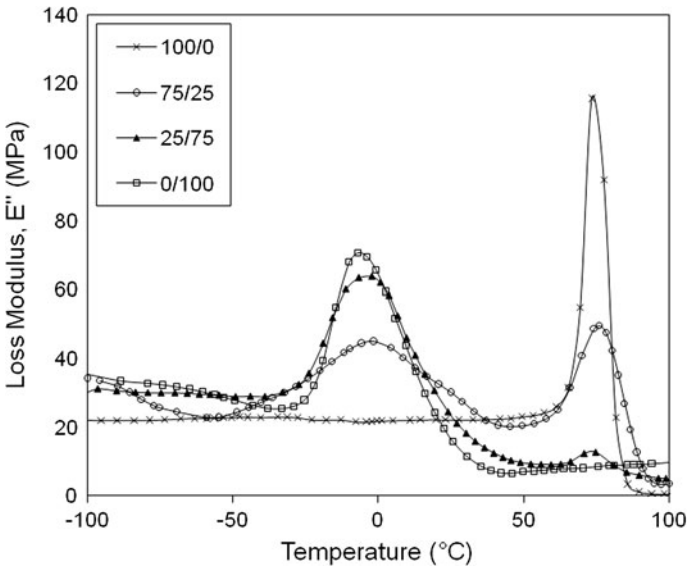

Fig. 5 Temperature dependence of loss moduli (E'') for neat PLLA, PBSL, and PLLA/PBSL blends

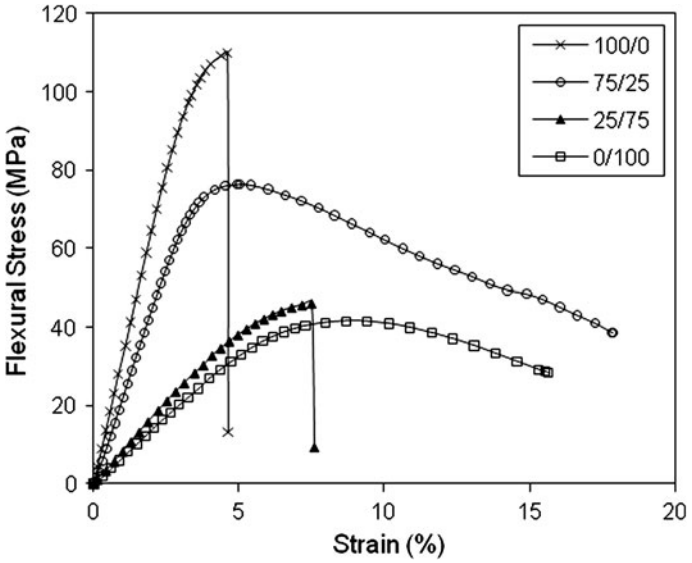

Fig. 6 Plot of flexural stress against strain for PLLA/PBSL blends with various blending ratios

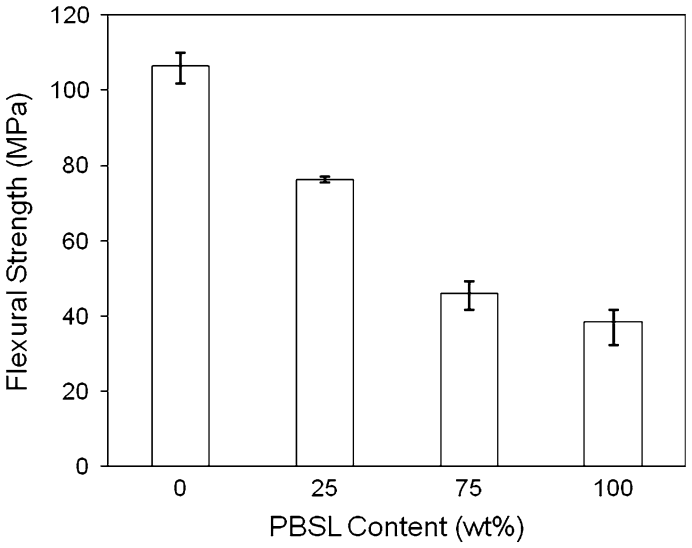

Fig. 7 Influence of PBSL content on the flexural strength of PLLA blends

under the graph of stress versus strain. Toughness is the property of a material that represents its capability to absorb energy before failure. From the stress–strain curves plotted, the toughness of the blends was found to increase with an increase in PBSL content. The neat PLLA and 25/75 blends exhibited brittle failure, in which the samples experienced no yielding before the break. On the other hand, plastic

deformations were observed in the neat PBSL and 75/25 blends, showing that both samples experienced ductile failure. The changes in flexural strength and modulus of the samples as a function of PBSL content are summarized in Figs. 7 and 8, respectively. In Fig. 7, the neat PLLA has the highest flexural strength and the addition of PBSL into the PLLA blends resulted in a gradual decrease in their flexural strength. To predict the flexural modulus of the PLLA/PBSL blends, Voigt and Reuss models were applied in this study. The Voigt model, which is also known as the upper bound parallel, is given by the following rule of mixture (Eq. 2) [25]:

$$E = E_1\varphi_1 + E_2\varphi_2, \tag{2}$$

where E is the modulus of the blend, E_1 and E_2 are the moduli of component 1 and 2, respectively, and φ_1 and φ_2 are the volume fractions of component 1 and 2, respectively. On the other hand, the Reuss model or the lower bound series is given by Eq. 3 [25]:

$$\frac{1}{E} = \frac{\varphi_1}{E_1} + \frac{\varphi_2}{E_2}. \tag{3}$$

Figure 8 shows that the experimental flexural modulus values are located in between the Voigt and Reuss models. However, the flexural modulus of the blend with PBSL content up to 25 wt% was close to the Voigt model's line. This suggests that compatibility between PLLA and PBSL is possible when PBSL content is less than 25 wt%. In addition, these flexural modulus values reduced with an increase of

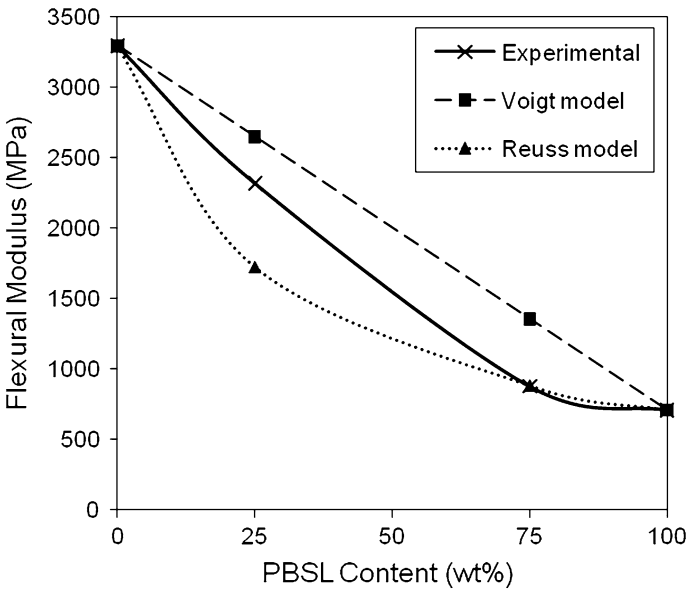

Fig. 8 Change in flexural modulus of PLLA blends as a function of PBSL content

PBSL content. This may be attributed to the decrease in degree of crystallinity of PLLA with increasing PBSL content [26, 27].

Morphological study

Figure 9 shows the field emission scanning electron micrographs of the fracture surface of the flexural test samples. A smooth fracture surface was observed in the neat PLLA, proving that it is brittle. In contrast, the fracture surface of PBSL was very rough, indicating that it is a ductile material that undergoes plastic deformation. It is obvious that the dispersed phase of PBSL in the sample with 75/25 blending ratio has relatively small mean diameter as compared to that of 25/75 blend. The result is in good agreement with the findings documented by Vilay et al. [19], wherein the increase of PBSL content resulted in an increase in the dispersed phase of PBSL. In addition, severe phase separation can be seen clearly in the 25/75 blend as shown in Fig. 9c, whilst the 75/25 blend (Fig. 9b) exhibited partial miscibility morphology. This is consistent with the flexural test result.

Based on the flexural properties observed, 75/25 blend was selected as the optimum blending ratio of PLLA and PBSL. The 75/25 blend was then annealed at 100 °C for different time periods. The following sections present the influences of annealing time on the properties of the blend.

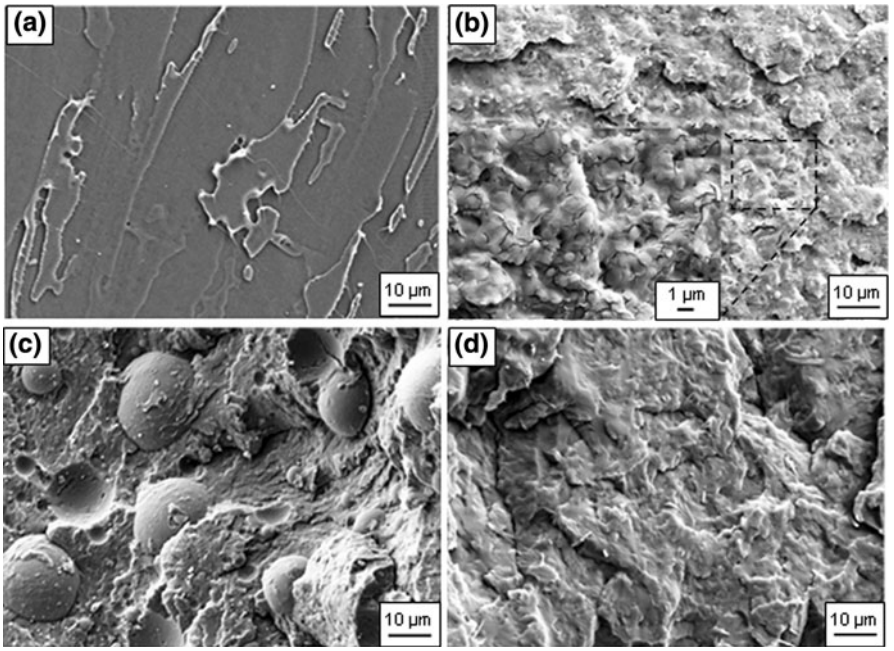

Fig. 9 FESEM images showing the fracture surface of **a** neat PLLA, **b** 75/25 blend, **c** 25/75 blend, and **d** neat PBSL

Effect of annealing time on the PLLA/PBSL blend

Thermal properties

The DSC thermograms of the annealed samples are shown in Fig. 10. Based on the DSC measurements presented in Table 3, the degree of crystallinity (X_c) of the blend evidently increased with an increase in annealing time. This was attributed to the reorientation of the macromolecular chains during annealing. As the annealing time increased, the number of polymer chains diffused into the proper orientations and increased the crystalline arrangement. Hence, the increase in annealing time resulted in an increase in the degree of blend crystallinity [28].

Mechanical properties

Figure 11 demonstrates the effect of annealing time on the flexural modulus and strength of the PLLA blend, respectively. Annealing resulted in an increase in the

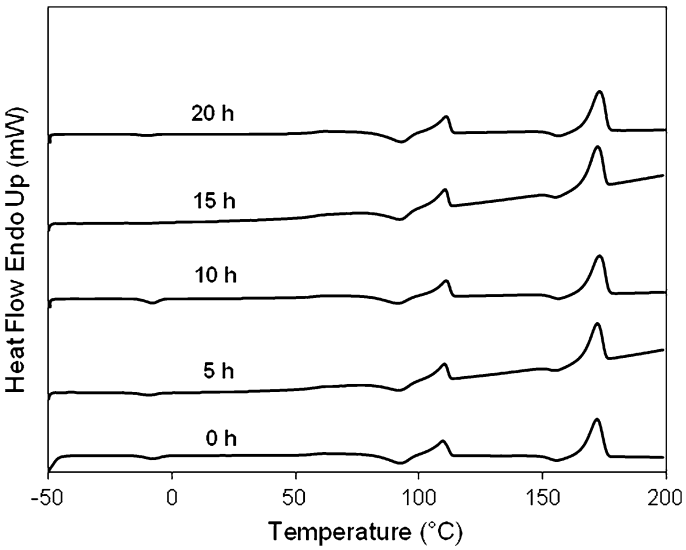

Fig. 10 DSC thermograms of 75/25 blend annealed at 100 °C for various time periods

Table 3 DSC measurements of annealed samples

Annealing time (h)	$T_{g,PLLA}$ (°C)	$T_{c,PLLA}$ (°C)	ΔH_c (J/g)	$T_{m,PLLA}$ (°C)	ΔH_m (J/g)	$X_{c,PLLA}$ (%)
0	57.75	92.49	−9.86	172.28	32.77	61.12
5	58.27	92.18	−10.20	172.49	33.10	62.08
10	58.35	91.13	−12.77	172.93	38.41	72.99
15	58.33	92.65	−13.61	172.56	37.71	73.58
20	58.49	92.62	−15.84	172.94	38.23	77.52

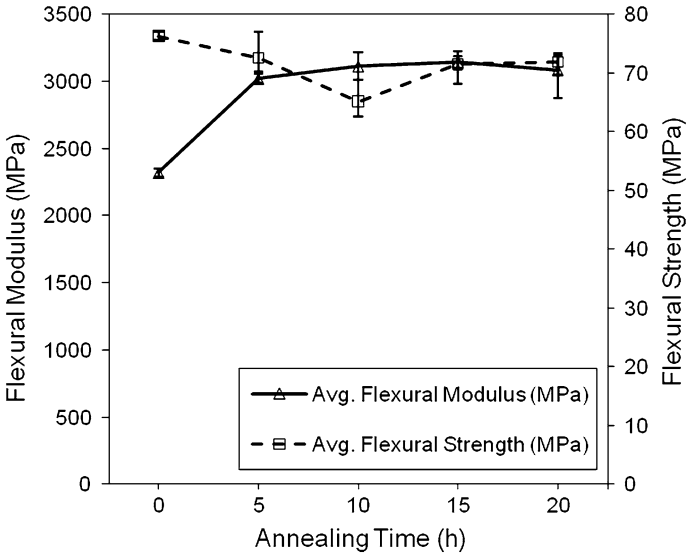

Fig. 11 Changes in flexural modulus and strength of 75/25 blend as a function of annealing time

flexural modulus of the blend. A drastic increase of flexural modulus about 30% was observed in the sample annealed for 5 h. Further increases in the annealing time resulted in a slight increase in the modulus of the blend. This was due to the change in crystallinity of the blend, as indicated in Table 3. According to Seymour and Carraher's findings, the modulus value is directly proportional to the degree of crystallinity [29]. Thus, the modulus of the sample is accepted to increase with an increase in annealing time. However, the modulus of the sample dropped slightly as the annealing time increased up to 20 h. This may be attributed to the thermal degradation of the polymer blend [13].

On the other hand, as the annealing time increased up to 10 h, the flexural strength of the blend was reduced to approximately 15% of that of unannealed 75/25

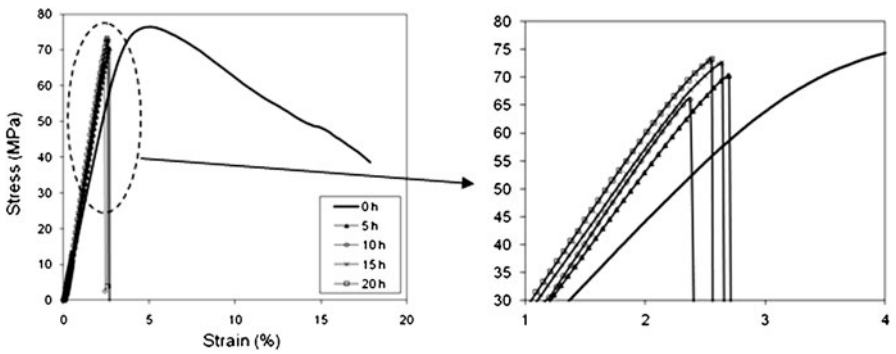

Fig. 12 Flexural stress against strain curves of 75/25 PLLA/PBSL blend annealed for various time

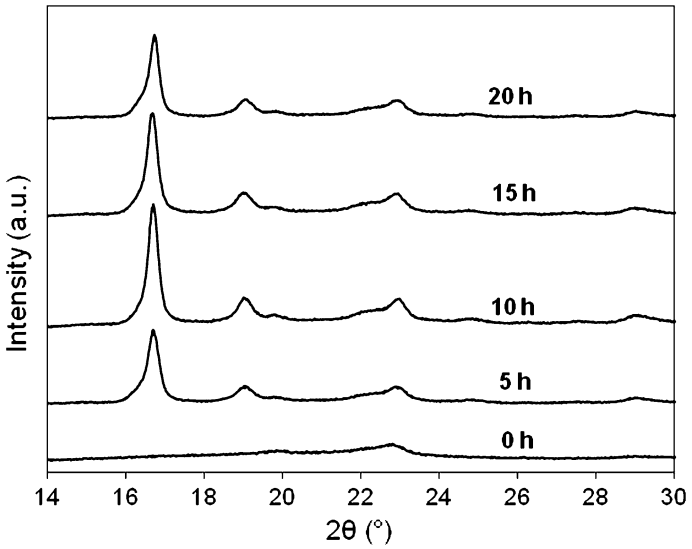

Fig. 13 XRD patterns of 75/25 blend with different annealing time

blend. A slight increase in flexural strength, however, was noted in samples annealed for 15 h and 20 h.

The stress against strain curves of the 75/25 blend annealed for various time is presented in Fig. 12. All annealed samples exhibited brittle behavior, whereas the sample without annealing showed ductile behavior. A ductile to brittle transition was observed during the annealing process. Moreover, the maximum strain of the blend was reduced from 17.88 to ~2.5% after annealing for 5 h. This was because of modifications to the crystal structure during annealing, which is supported by the XRD results shown in Fig. 13.

X-ray diffraction (XRD) analysis

As observed in Fig. 13, the XRD patterns of the annealed samples are completely different from those of the unannealed sample. Three crystalline peaks were clearly seen in the XRD patterns of the annealed samples, a sharp peak at 2θ of 16.8° and two smaller peaks at 2θ of 19.1° and 23°. In contrast, the XRD pattern of the 75/25 blend without annealing exhibited only one small peak at 2θ of 23°, indicating the characteristic peak of the sample. The intensity of the crystalline peaks increased with an increase in annealing time. This was attributed to the development of more ordered crystallites and the formation of more crystalline structures after annealing [30].

Conclusion

Blending PLLA with PBSL reduced the brittleness of neat PLLA. The addition of PBSL improved the toughness of PLLA blends. The thermal stability of the blend

was enhanced with an increase in PBSL content. In DMA, the PLLA/PBSL blends exhibited two T_g's, indicating that PBSL is partially miscible with PLLA. Annealing resulted in an improvement in the degree of crystallinity, as well as the flexural modulus, of the PLLA/PBSL blend. In future work, a novel compatibilizer can be synthesized and added into the PLLA blend to improve its miscibility.

Acknowledgments The authors would like to acknowledge the Ministry of Higher Education Malaysia and Universiti Sains Malaysia for providing us USM-RU-PRGS research grant (no. 8043044), USM Fellowship and research facilities.

References

1. Drumright RE, Gruber PR, Henton DE (2000) Polylactic acid technology. Adv Mater 12(23): 1841–1846
2. Garlotta R (2001) A literature review of poly(lactic acid). J Polym Environ 9(2):63–84
3. Wang SG (1997) Classification, synthesis and application of biodegradable polymer. Chem Commun 2:45–47
4. Hunneault MA, Li HB (2007) Morphology and properties of compatibilized polylactide/thermoplastic starch blends. Polymer 48(1):270–280
5. Aslan S, Calandrelli L, Laurienzo P, Malinconico M, Migliaresi C (2000) Poly(D,L-lactic acid)/poly(caprolactone) blend membranes: preparation and morphological characterization. J Mater Sci 35:1615–1622
6. Ikehara T, Nishikawa Y, Nishi T (2003) Evidence for the formation of interpenetrated spherulites in poly(butylene succinate-*co*-butylene carbonate)/poly(L-lactic acid) blends investigated by atomic force microscopy. Polymer 44(21):6657–6661
7. Cao X, Mohamed A, Gordon SH, Willett JL, Sessa DJ (2003) DSC study of biodegradable poly(lactic acid) and poly(hydroxy ester ether) blends. Thermochim Acta 406(1–2):115–127
8. Shibata M, Inoue Y, Miyoshi M (2006) Mechanical properties, morphology, and crystallization behavior of blends of poly(L-lactide) with poly(butylene succinate-*co*-L-lactate) and poly(butylene succinate). Polymer 47:3557–3564
9. Bhatia A, Gupta RK, Bhattacharya SN, Choi HJ (2007) Compatibility of biodegradable poly (lactic acid) (PLA) and poly (butylene succinate) (PBS) blends for packaging application. Korea-Aust Rheol J 19(3):125–131
10. Park JW, Im SS (2002) Phase behavior and morphology in blends of poly(L-lactic acid) and poly(butylene succinate). J Appl Polym Sci 86:647–655
11. Yokohara T, Yamaguchi M (2008) Structure and properties for biomass-based polyester blends of PLA and PBS. Eur Polym J 44:677–685
12. Shay RM Jr, Caruther JM (1990) A predictive model for the effects of thermal history on the mechanical behavior of amorphous polymers. Polym Eng Sci 30:1266–1280
13. Tsuji H, Ikada Y (1995) Properties and morphologies of poly(L-lactide): 1. Annealing condition effects on properties and morphologies of poly(L-lactide). Polymer 36(14):2709–2716
14. Huda MS, Yasui M, Mohri N, Fujimura T, Kimura Y (2002) Dynamic mechanical properties of solution-cast poly(L-lactide) films. Mater Sci Eng A333:98–105
15. Kobayashi S, Kogo Y (2007) Effect of heat treatment on the mechanical and fracture properties of poly(lactic acid)/poly(butylenes succinate) blends. Trans Jpn Soc Mech Eng Ser A 73(729):589–594
16. Fischer EW, Sterzel HJ, Wegner G, Kolloid ZZ (1973) Investigation of the structure of solution grown crystals of lactide copolymers by means of chemical reaction. Polymer 251:980–990
17. ASTM D790-03 (2005) Standard test method for flexural properties of unreinforced and reinforced plastics and electrical insulating materials. The American Society for Testing and Materials, Annual Book of ASTM Standards 08.01, Philadelphia, pp 149–159
18. Mehta A, Isayev A (1991) Rheology, morphology, and mechanical characteristics of poly(etherether ketone)-liquid crystal polymer blends. Polym Eng Sci 31(13):971–980
19. Vilay V, Mariatti M, Zulkifli A, Todo M (2009) Characterization of the mechanical and thermal properties and morphological behavior of biodegradable poly(L-lactide)/poly(ε-caprolactone) and

poly(L-lactide)/poly(butylene succinate-*co*-L-lactate) polymeric blends. J Appl Polym Sci 114: 1784–1792
20. Zhang J, Duan Y, Sato H, Tsuji H, Noda I, Yan S, Ozaki Y (2005) Crystal modifications and thermal behavior of poly(L-lactic acid) revealed by infrared spectroscopy. Macromolecules 38:8012
21. Zhang GY, Ma JW, Cui BX, Ma DZ (2001) Compatibilizing effect of transesterification copolymers on bisphenol A polycarbonate/poly(ethylene terephthalate) blends. Macromol Chem Phys 202: 604–613
22. Kong Y, Hay JN (2002) Miscibility and crystallisation behaviour of poly(ethylene terephthalate)/ polycarbonate blends. Polymer 43:1805–1811
23. Okamoto K, Ichikawa T, Yokohara T, Yamaguchi M (2009) Miscibility, mechanical and thermal properties of poly(lactic acid)/polyester-diol blends. Eur Polym J 45:2304–2312
24. Hatakeyama T (1994) Thermal analysis: fundamentals and applications to polymer science. John Wiley & Sons, New York
25. Nielsen LE, Landel RF (1994) Mechanical properties of polymer and composites. Marcel Dekker, New York
26. El-Hadi A, Schnabel R, Straube E, Müller G, Henning S (2002) Correlation between degree of crystallinity, morphology, glass temperature, mechanical properties and biodegradation of poly (3-hydroxyalkanoate) PHAs and their blends. Polym Test 21(6):665–674
27. Liu X, Dever M, Fair N, Benson RS (1997) Thermal and mechanical properties of poly(lactic acid) and poly(ethylene/butylene succinate) blends. J Environ Polym Degrad 5(4):225–235
28. Munk P, Aminabhavi TM (2002) Introduction to macromolecular science. Wiley, New York
29. Seymour RB, Carraher CE (1984) Structure–property relationship in polymers. Plenum Press, New York
30. Kim JY, Seo ES, Kim SH (2003) Effects of annealing on structure and properties of TLCP/PEN/PET ternary blend fibers. Macromol Res 11(1):62–68